Dynamical properties of entry games with firms adopting different adjustment mechanisms

Xiaoliang Li[*a,b] and Ally Quan Zhang[†c]

[a]MoE Key Laboratory of Interdisciplinary Research of Computation and Economics, Shanghai University of Finance and Economics, Shanghai 200433, China

[b]School of Business, Guangzhou College of Technology and Business, Guangzhou 510850, China

[c]Department of Accounting and Finance, Lancaster University Management School, Lancaster LA1 4YX, United Kingdom

Abstract

This paper investigates the dynamical properties of three entry games in a market initially composed of N gradient-adjusting firms. The entrant may adopt one of three output adjustment mechanisms: gradient adjustment, best response, or local monopolistic approximation (LMA). Under the assumptions that the entrant's marginal cost does not differ significantly from the average marginal cost of the incumbents and that the number of incumbent firms is no less than four, we establish an ordering of the stability regions, indicating that less information in the adjustment mechanism may lead to stronger market stability. With respect to dynamics, we find that the entry model of a best response firm differs qualitatively from the other two. Furthermore, numerical simulations reveal that this model may exhibit 1:3, 1:4, and 1:5 resonance bifurcations, and may also display the coexistence of multiple attractors.

Keywords: Cournot competition; entry game; oligopoly model; isoelastic demand; local stability; bifurcation

[*]xiaoliangbuaa@gmail.com

[†]q.zhang20@lancaster.ac.uk

1 Introduction

Since the pioneering work of Cournot [1] on the framework of oligopolistic competition, the stability analysis of oligopoly games has long been a central issue in microeconomics. For instance, Theocharis [2] made seminal contributions to the study of stability in the Cournot model. He assumed that the market is characterized by a linear demand function, all competing firms know the explicit form of this demand, and each firm faces a linear cost function. Under these assumptions, Theocharis constructed a discrete dynamical model and demonstrated that the equilibrium is stable when the number of firms does not exceed three, but instability arises when the number of competitors exceeds this threshold.

Fisher [3], McManus and Quandt [4] extended Theocharis's work by retaining the assumption of linear demand while relaxing the linear cost assumption. Sato and Nagatani [5] modified the original Cournot framework by relaxing the assumption that each firm expects its rivals to maintain their previous output levels. They proposed a conjectural variation model that more closely reflects actual market behaviors and analyzed its stability. Hadar [6] employed discrete dynamical systems to describe differentiated-product oligopolies and provided sufficient (though not necessary) conditions for system stability. In a related vein, Zhang and Zhang [7] developed a model in which each firm sells multiple products across several markets. They derived necessary and sufficient conditions for the Nash equilibrium to be locally stable and discussed how these stability results can be applied to comparative statics across different oligopolistic markets.

Since the 1990s, the focus of mathematical economists has gradually shifted from studying the stability of oligopolistic games to exploring their complex dynamical behaviors, with particular attention given to various output adjustment mechanisms. For example, Puu [8] examined a nonlinear-demand duopoly market, where both firms only observe each other's output from the previous period and naively expect their rivals to produce the same quantity in the current period. In Puu's model, firms adjust their outputs according to the best response functions that maximize their expected profits. Bischi and Kopel [9], Wu et al. [10] analyzed adaptive players who determine their current outputs based on a weighted combination of their own previous output and the best response derived from naive expectations about their competitors' behaviors. Bischi et al. [11] introduced the *Local Monopolistic Approximation* (LMA) mechanism, in which firms linearly approximate the demand function and adjust their output accordingly.

They demonstrated that less information may lead to greater stability of the equilibrium. A similar conclusion was reached by Naimzada and Sbragia [12], who showed that a duopoly game with LMA dynamics is globally stable. In addition, Xin et al. [13] investigated a discrete fractional-order Cournot duopoly game, where firms possess long-term memory of their past output decisions and determine their current strategies by fully utilizing historic information.

The studies mentioned above predominantly assume that firms rely on homogeneous adjustment mechanisms. More recent research has shifted attention toward the implications of heterogeneity in firms' adjustment behaviors. For example, Agiza and Elsadany [14] analyzed a nonlinear discrete-time Cournot duopoly model in which firms adopt boundedly rational and naive expectation rules. Tramontana et al. [15] examined the influence of heterogeneous expectations in a setting with a nonlinear demand function, where each firm employs a distinct expectation-formation mechanism. They found that such heterogeneity may enhance the stability of the equilibrium. Cavalli and Naimzada [16] studied duopolistic competition with heterogeneous players characterized by two types of adjustment mechanisms, each reflecting a relatively low degree of rationality. Cavalli et al. [17] subsequently investigated general oligopolies composed of heterogeneous firms that adjust their outputs according to best response mechanisms based either on perfect foresight or static expectations. Their results suggest that a higher degree of rationality does not necessarily lead to improved stability, particularly when the marginal cost of the more rational firms is sufficiently high. Matouk et al. [18] proposed a nonlinear oligopoly model with four fully heterogeneous firms. They demonstrated that the system may lose stability through both period-doubling and Neimark–Sacker bifurcations, along with exhibiting the coexistence of multiple chaotic attractors. Furthermore, Elsadany and Awad [19] compared price and quantity competition in a mixed duopoly model subject to environmental taxation, where heterogeneous adjustment mechanisms are adopted by firms.

The entry game lies at the core of industrial organization theory, as it reveals how market structure is endogenously determined by firms' entry decisions and strategic interactions, thereby serving as a fundamental framework linking market theory, competition policy, and the analysis of industry dynamics. In the existing literature, there are very few studies on the stability of entry games. To the best of our knowledge, this paper represents the first attempt in this direction.

Under the setting of an isoelastic demand market with N gradient-adjusting incumbent

firms, we examine the dynamical properties of a new firm entering the market. In our framework, the entrant may adopt one of three different mechanisms for adjusting its output—namely the gradient adjustment, best response, and LMA mechanisms—leading to the following three entry games:

1. Entry of a gradient-adjusting firm;
2. Entry of a best response firm;
3. Entry of an LMA firm.

We establish the local stability conditions for the above three entry games. Under reasonable assumptions, we derive the relative sizes of the stability regions corresponding to these models. By abuse of notation, the stability regions resulting from the entry of different types of firms can be ordered as follows:

Entry of a best response firm $\preceq$ Entry of an LMA firm $\preceq$ Entry of a gradient-adjusting firm.

The remainder of this paper is organized as follows. In Section 2, we set up a market with N firms, each employing the gradient mechanism to adjust its output. Section 3 examines the problem of a new firm entering this N-firm market, where the entrant may adopt one of three different adjustment strategies: gradient adjustment, best response, or LMA, corresponding to three distinct models. Section 4 compares the sizes of the stability regions for these three models. In Section 5, we conduct numerical simulations to explore the complex dynamics of the models. Finally, Section 6 concludes the study.

2 Market with N Gradient-Adjusting Firms

Consider a market with N firms ($N \geq 2$), where the output of firm i is denoted by q_i. The cost function of firm i is given by $C_i(q_i) = c_i q_i$, with $c_i > 0$. We denote the previous period by t and the current period by $t+1$.

In the literature, linear demand functions are often employed for analytical convenience. However, in this study, we adopt a nonlinear demand function for two reasons. First, empirical studies have frequently found that linear specifications are not supported and nonlinearities

are commonly observed.[1] Second, employing a nonlinear demand function leads to a nonlinear marginal profit function, which in turn yields a nonlinear discrete dynamical system. In this case, the corresponding dynamical system may exhibit rich dynamical behaviors, thereby offering greater research value from a mathematical perspective.

Following [8, 22], we assume that the inverse demand function is isoelastic, i.e.,

$$P(Q) = \frac{1}{Q},$$

where $Q = \sum_{i=1}^{N} q_i$ denotes the market supply or aggregate output. Accordingly, the profit function of firm i in period t is given by

$$\Pi_i(t) = \frac{q_i(t)}{Q(t)} - c_i q_i(t),$$

and the marginal profit with respect to $q_i(t)$ is

$$\frac{\partial \Pi_i(t)}{\partial q_i(t)} = \frac{1}{Q(t)} - \frac{q_i(t)}{Q^2(t)} - c_i.$$

We suppose that firm i dynamically adjusts its output according to the *gradient adjustment mechanism* [23, 24]. Specifically, firm i determines its output for period $t+1$ according to

$$q_i(t+1) = q_i(t) + k_i \left(\frac{1}{Q(t)} - \frac{q_i(t)}{Q^2(t)} - c_i \right),$$

where $k_i > 0$ denotes the adjustment speed. For the sake of simplicity, we assume $k_i = k$ for all firms throughout the remainder of this paper. Thus,

$$q_i(t+1) = q_i(t) + k \left(\frac{1}{Q(t)} - \frac{q_i(t)}{Q^2(t)} - c_i \right). \tag{1}$$

By summing Eq. (1) over $i = 1, \ldots, N$, we obtain the aggregate map

$$Q(t+1) = Q(t) + k \left(\frac{N-1}{Q(t)} - \sum_{i=1}^{N} c_i \right), \tag{2}$$

[1]For instance, Ng [20] employed threshold autoregressive models to analyze commodity price data and provided evidence of nonlinearities in prices. Similarly, Adrangi and Chatrath [21] found strong evidence of nonlinear dependence and noted that well-known Autoregressive Conditional Heteroskedasticity (ARCH) processes can generally account for the observed nonlinearities, provided that the effects of seasonality and contract maturity are appropriately controlled.

where $\sum_{i=1}^{N} c_i > 0$ denotes the aggregate marginal cost.

Proposition 1. *The equilibrium output of firm i is given by*

$$q_i^* = \frac{(N-1)\left(\sum_{i=1}^{N} c_i + c_i - Nc_i\right)}{\left(\sum_{i=1}^{N} c_i\right)^2}.$$

Proof. Setting $Q(t+1) = Q(t) = Q^*$ in (2) yields

$$Q^* = Q^* + k\left(\frac{N-1}{Q^*} - \sum_{i=1}^{N} c_i\right),$$

which implies

$$Q^* = \frac{N-1}{\sum_{i=1}^{N} c_i},$$

since $k > 0$.

Furthermore, by setting $Q(t+1) = Q(t) = Q^*$ and $q_i(t+1) = q_i(t) = q_i^*$ in (1), we obtain

$$q_i^* = Q^* - c_i Q^{*2} = \frac{Q^*\left(\sum_{i=1}^{N} c_i + c_i - Nc_i\right)}{\sum_{i=1}^{N} c_i} = \frac{(N-1)\left(\sum_{i=1}^{N} c_i + c_i - Nc_i\right)}{\left(\sum_{i=1}^{N} c_i\right)^2}.$$

This completes the proof. □

From Proposition 1, it follows that for $i \neq j$,

$$\frac{q_i^*}{q_j^*} = \frac{\sum_{i=1}^{N} c_i - c_i(N-1)}{\sum_{i=1}^{N} c_i - c_j(N-1)}.$$

This implies $q_i^* < q_j^*$ if $c_i > c_j$. In other words, a more efficient firm, i.e., one with lower marginal costs, will produce larger output and hold a greater market share.

The aggregate map (2) is locally stable if

$$-1 < \frac{\partial Q(t+1)}{\partial Q(t)}\Big|_{Q^*} < 1,$$

where

$$\frac{\partial Q(t+1)}{\partial Q(t)}\Big|_{Q^*} = 1 - k\frac{N-1}{(Q^*)^2} = 1 - k\frac{\left(\sum_{i=1}^{N} c_i\right)^2}{N-1}.$$

Clearly, $\frac{\partial Q(t+1)}{\partial Q(t)}\Big|_{Q^*} < 1$ always holds. Hence, the local stability condition of the equilibrium point reduces to

$$k < \frac{2(N-1)}{\left(\sum_{i=1}^{N} c_i\right)^2}.$$

Let a denote the average marginal cost of the N firms, i.e.,

$$a \equiv \frac{\sum_{i=1}^{N} c_i}{N} > 0.$$

Accordingly, the stability condition can be expressed as

$$k < \frac{2(N-1)}{(aN)^2}. \tag{3}$$

It can be observed that as N increases, the right-hand side of inequality (3) decreases, making it more difficult to stabilize the equilibrium point. In other words, the number of firms N acts as a destabilizing factor. Similarly, it is evident that both the adjustment speed k and the average marginal cost a also serve as destabilizing factors.

A number of natural and interesting questions arise. When a new firm enters the market already populated by N gradient-adjusting firms, how will the stability of the equilibrium change? Is it possible for the stability region in the parameter space to expand? In the next section, we will consider three different types of potential entrants, each characterized by a distinct output adjustment mechanism. Which type of entrant is more conducive to the stability of the equilibrium?

3 Entry Games

In this section, we consider the entry of a new firm into the N-firm market described in the previous section. The entrant may follow one of three output adjustment mechanisms: the gradient adjustment mechanism, the best response mechanism, or the LMA mechanism. This gives rise to an extended model, for which we will analyze the local stability of its equilibrium.

Let the output of the entrant be denoted by q_s, and assume that its cost function is $C(q_s) = cq_s$ with $c > 0$.

3.1 Entry of a gradient-adjusting firm

We denote by Q_N the aggregate output of the first N firms, all of which follow the gradient adjustment mechanism. For $i = 1, \ldots, N$, the dynamics of each firm are described by

$$q_i(t+1) = q_i(t) + k\left(\frac{1}{Q_N(t) + q_s(t)} - \frac{q_i(t)}{(Q_N(t) + q_s(t))^2} - c_i\right),$$

which implies that the aggregate output evolves according to

$$Q_N(t+1) = Q_N(t) + k\left(\frac{N}{Q_N(t) + q_s(t)} - \frac{Q_N(t)}{(Q_N(t) + q_s(t))^2} - aN\right),$$

where $a = \frac{\sum_{i=1}^{N} c_i}{N} > 0$ denotes the average marginal cost of the first N firms.

Suppose that the entrant also adopts the *gradient adjustment mechanism*, with the same adjustment speed k. Then, the resulting $(N+1)$-firm model, which we denote by NG1G, can be expressed as the following discrete dynamical system:

$$\begin{cases} Q_N(t+1) = Q_N(t) + k\left(\dfrac{N}{Q_N(t) + q_s(t)} - \dfrac{Q_N(t)}{(Q_N(t) + q_s(t))^2} - aN\right), \\ q_s(t+1) = q_s(t) + k\left(\dfrac{1}{Q_N(t) + q_s(t)} - \dfrac{q_s(t)}{(Q_N(t) + q_s(t))^2} - c\right), \end{cases} \tag{4}$$

where c is the entrant's marginal cost.

By setting $Q_N(t+1) = Q_N(t) = Q_N^*$ and $q_s(t+1) = q_s(t) = q_s^*$, we obtain the equilibrium equations as follows:

$$\begin{cases} Q_N^* = Q_N^* + k\left(\dfrac{N}{Q_N^* + q_s^*} - \dfrac{Q_N^*}{(Q_N^* + q_s^*)^2} - aN\right), \\ q_s^* = q_s^* + k\left(\dfrac{1}{Q_N^* + q_s^*} - \dfrac{q_s^*}{(Q_N^* + q_s^*)^2} - c\right), \end{cases}$$

which can be explicitly solved by

$$Q_N^* = \frac{cN^2}{(aN + c)^2}, \qquad q_s^* = \frac{N\,(aN + c - cN)}{(aN + c)^2}.$$

From an economic perspective, the parameters must ensure that the equilibrium outputs are non-negative to be meaningful; we refer to such parameters as *feasible parameters*. From the above closed-form solution of the equilibrium, it is clear that $Q_N^* \geq 0$ always holds, while

$q_s^* \geq 0$ if and only if

$$\frac{a}{c} \geq \frac{N-1}{N}.$$

In other words, the feasible parameter set requires that the average marginal cost of the first N incumbent firms is not smaller than $(N-1)/N$ times the marginal cost of the entrant.

The Jacobian matrix of map (4) is

$$\mathbf{J} = \begin{bmatrix} 1 + k\left(-\dfrac{N+1}{(Q_N(t)+q_s(t))^2} + \dfrac{2Q_N(t)}{(Q_N(t)+q_s(t))^3}\right) & k\left(-\dfrac{N}{(Q_N(t)+q_s(t))^2} + \dfrac{2Q_N(t)}{(Q_N(t)+q_s(t))^3}\right) \\ k\left(-\dfrac{1}{(Q_N(t)+q_s(t))^2} + \dfrac{2q_s(t)}{(Q_N(t)+q_s(t))^3}\right) & 1 + k\left(-\dfrac{2}{(Q_N(t)+q_s(t))^2} + \dfrac{2q_s(t)}{(Q_N(t)+q_s(t))^3}\right) \end{bmatrix}.$$

By plugging the closed-form solution, we derive the Jacobian matrix at the equilibrium, i.e.,

$$\mathbf{J}^* = \begin{bmatrix} 1 - \dfrac{k\left((aN-c)N + aN + c\right)(aN+c)}{N^2} & -\dfrac{k\left(a^2N^2 - c^2\right)}{N} \\ \dfrac{k\left((a-2c)N + c\right)(aN+c)}{N^2} & \dfrac{-2Nack - 2c^2k + N}{N} \end{bmatrix}.$$

Theorem 1. *The equilibrium of model NG1G is locally stable if*

$$k < \frac{2N}{(aN+c)^2}. \tag{5}$$

Furthermore, the equilibrium may undergo period-doubling bifurcations when

$$k = \frac{2N}{(aN+c)^2}.$$

Proof. The two eigenvalues of the Jacobian matrix $\mathbf{J}^*$ are real and given by

$$\lambda_1 = 1 - \frac{k(aN+c)^2}{N^2}, \qquad \lambda_2 = 1 - \frac{k(aN+c)^2}{N}.$$

Since $N \geq 2$ and $k > 0$, it is evident that $\lambda_2 < \lambda_1 < 1$. The equilibrium of model NG1G is locally stable if $\lambda_2 > -1$, which is equivalent to condition (5). According to classical bifurcation theory, the equilibrium may undergo period-doubling bifurcations when $\lambda_2 = -1$. This completes the proof. □

By comparing conditions (3) and (5), it follows that the stability region expands upon the

entry of a gradient-adjusting firm if and only if

$$\frac{N-1}{(aN)^2} < \frac{N}{(aN+c)^2}.$$

This is equivalent to

$$\left(\frac{aN+c}{aN}\right)^2 < \frac{N}{N-1},$$

which can be further simplified as

$$\frac{c}{a} < N\sqrt{\frac{N}{N-1}} - N.$$

Remark 1. Therefore, we may assert that if the entrant's marginal cost c is sufficiently low relative to the incumbents' average marginal cost a, the $(N+1)$-firm market will exhibit stronger stability than the original N-firm market. The economic implication is that, given that the entrant adopts the gradient adjustment mechanism, a sufficiently efficient entrant can enhance overall market stability. This insight may be informative for regulators when designing market entry policies.

In addition, this result is related to the findings of Tramontana et al. [15]. By gradually introducing heterogeneous firms, Tramontana et al. showed that heterogeneity in firms' decision-making mechanisms may enhance market stability. In contrast, our results demonstrate that when all firms adopt a homogeneous adjustment rule—namely, the gradient adjustment mechanism—the entry of a sufficiently efficient firm (i.e., a firm with a sufficiently low marginal cost) can also enhance market stability. □

Figure 1 presents several cross-sections of the stability region for model NG1G, where the yellow areas represent the stable region, and the grey areas correspond to the infeasible parameter region ($q_s^* < 0$). In addition, the blue curves indicate the period-doubling bifurcation curves, while the green lines represent the stability boundaries of the N-firm market (the market is stable on the left side of the green lines).

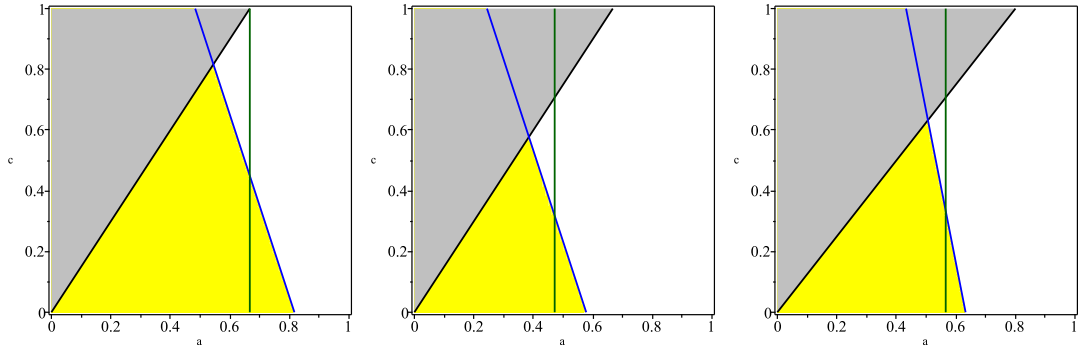

(a) $N = 3$, $k = 1$ (b) $N = 3$, $k = 2$ (c) $N = 5$, $k = 1$

Figure 1: Stability region of model NG1G.

3.2 Entry of a best response firm

Suppose that the entrant adopts the *best response mechanism* [8, 25]. Specifically, the entrant forms a naive expectation for period $t + 1$ that the other firms will produce the same output quantities as in period t. Then, the expected profit of the entrant for period $t + 1$ is given by

$$\Pi^e(t+1) = \frac{q_s(t+1)}{Q_N(t) + q_s(t+1)} - cq_s(t+1),$$

where c is the entrant's marginal cost.

To maximize the expected profit, we have the following first-order condition:

$$\frac{\partial \Pi^e(t+1)}{\partial q_s(t+1)} = \frac{Q_N(t)}{(Q_N(t) + q_s(t+1))^2} - c = 0.$$

The second-order condition is always satisfied since

$$\frac{\partial^2 \Pi^e(t+1)}{\partial q_s^2(t+1)} = -\frac{2Q_N(t)}{(Q_N(t) + q_s(t+1))^3} \leq 0.$$

Solving the first-order condition yields

$$q_s(t+1) = -Q_N(t) + \sqrt{\frac{Q_N(t)}{c}},$$

which is referred to as the *best response function* of the entrant.

Then the new model with $N + 1$ firms, which we call model NG1B, can be formulated as

the following map:

$$\begin{cases} Q_N(t+1) = Q_N(t) + k\left(\dfrac{N}{Q_N(t)+q_s(t)} - \dfrac{Q_N(t)}{(Q_N(t)+q_s(t))^2} - aN\right), \\ q_s(t+1) = -Q_N(t) + \sqrt{\dfrac{Q_N(t)}{c}}. \end{cases} \tag{6}$$

By setting $Q_N(t+1) = Q_N(t) = Q_N^*$ and $q_s(t+1) = q_s(t) = q_s^*$, we obtain the equilibrium equations as follows:

$$\begin{cases} Q_N^* = Q_N^* + k\left(\dfrac{N}{Q_N^*+q_s^*} - \dfrac{Q_N^*}{(Q_N^*+q_s^*)^2} - aN\right), \\ q_s^* = -Q_N^* + \sqrt{\dfrac{Q_N^*}{c}}. \end{cases}$$

It can be verified that the solution is given by

$$Q_N^* = \frac{cN^2}{(aN+c)^2}, \quad q_s^* = \frac{N(aN+c-cN)}{(aN+c)^2}.$$

Notice that the above equilibrium coincides with that of model NG1G. Therefore, model NG1B shares the same feasible parameter region, namely

$$\{(N,k,a,c) : N \geq 2,\ k > 0,\ a > 0,\ c > 0,\ a/c \geq (N-1)/N\}.$$

The Jacobian matrix of map (6) is

$$\mathbf{J} = \begin{bmatrix} 1 + k\left(-\dfrac{N+1}{\left(Q_N(t)+q_s(t)\right)^2} + \dfrac{2Q_N(t)}{\left(Q_N(t)+q_s(t)\right)^3}\right) & k\left(-\dfrac{N}{\left(Q_N(t)+q_s(t)\right)^2} + \dfrac{2Q_N(t)}{\left(Q_N(t)+q_s(t)\right)^3}\right) \\ -1 + \dfrac{1}{2\sqrt{cQ_N(t)}} & 0 \end{bmatrix}.$$

Accordingly, we derive the Jacobian matrix at the equilibrium, i.e.,

$$\mathbf{J}^* = \begin{bmatrix} 1 - \dfrac{k\left((aN-c)N + aN + c\right)(aN+c)}{N^2} & -\dfrac{k\left(a^2N^2 - c^2\right)}{N} \\ -1 + \dfrac{aN+c}{2cN} & 0 \end{bmatrix}.$$

The two eigenvalues of $\mathbf{J}^*$ are $\frac{\alpha_1 \pm \sqrt{\beta_1}}{2N^2c}$, where

$$\alpha_1 = k(N-1)c^3 - 2Nkac^2 - N^2\left(Na^2k + ka^2 - 1\right)c,$$

and

$$\beta_1 = c\left((aN+c)^2 c\left(aN^2+(a-c)N+c\right)^2 k^2 - 2(aN+c)N^3\left(a(a-c)N+c(a+c)\right)k + N^4 c\right).$$

A simple analysis shows that β_1 may be either positive or negative, which implies that the eigenvalues can be either real or complex. As a result, determining the stability of the model by directly checking whether the moduli of the eigenvalues lie inside the unit circle is rather cumbersome. However, a more convenient approach can be obtained by applying the Jury's criterion provided in the following lemma [26].

Lemma 1 (Jury's criterion)**.** *Let the Jacobian matrix at an equilibrium be given by*

$$\mathbf{J}^* = \begin{bmatrix} J_{11} & J_{12} \\ J_{21} & J_{22} \end{bmatrix}.$$

We denote

$$\begin{aligned} &\mathrm{Tr}(\mathbf{J}^*) \equiv J_{11} + J_{22}, \\ &\mathrm{Det}(\mathbf{J}^*) \equiv J_{11}J_{22} - J_{12}J_{21}, \end{aligned}$$

which are called the trace *and* determinant *of* $\mathbf{J}^*$*, respectively. Then the considered equilibrium is locally stable if*

$$\begin{aligned} &CD_1 \equiv 1 - \mathrm{Tr}(\mathbf{J}^*) + \mathrm{Det}(\mathbf{J}^*) > 0, \\ &CD_2 \equiv 1 + \mathrm{Tr}(\mathbf{J}^*) + \mathrm{Det}(\mathbf{J}^*) > 0, \\ &CD_3 \equiv 1 - \mathrm{Det}(\mathbf{J}^*) > 0. \end{aligned}$$

Theorem 2. *The equilibrium of model NG1B is locally stable if* $R_1 > 0$ *and* $R_2 > 0$*, where*

$$\begin{aligned} R_1 &= (Na+c)\left(a(a-4c)N^2 - 2c(a-2c)N - 3c^2\right)k + 4N^2 c, \\ R_2 &= -(Na+c)(Na-c)\left((a-2c)N+c\right)k + 2N^2 c. \end{aligned}$$

Furthermore, the equilibrium may undergo period-doubling and Neimark–Sacker bifurcations when $R_1 = 0$ *and* $R_2 = 0$*, respectively.*

Proof. We verify the three conditions provided in Lemma 1 sequentially, yielding

$$CD_1 = \frac{k(aN+c)^3}{2N^2c}, \quad CD_2 = \frac{R_1}{2N^2c}, \quad CD_3 = \frac{R_2}{2N^2c}.$$

It is evident that $CD_1 > 0$ always holds. Moreover, $CD_2 > 0$ and $CD_3 > 0$ are equivalent to $R_1 > 0$ and $R_2 > 0$, respectively. The conclusions regarding bifurcations then directly follow from the classical bifurcation theory. This completes the proof. □

Both conditions $R_1 > 0$ and $R_2 > 0$ given in Theorem 2 are necessary, since the satisfaction of one condition does not imply the other. For instance, when $N = 2$, $k = 1$, $a = 0.8$, and $c = 0.2$, we have $R_1 = 2.408 > 0$ but $R_2 = -0.92 < 0$, which shows that $R_1 > 0 \not\Rightarrow R_2 > 0$. Similarly, when $N = 2$, $k = 1$, $a = 0.8$, and $c = 0.6$, we have $R_2 = 5.24 > 0$ but $R_1 = -1.928 < 0$, indicating that $R_2 > 0 \not\Rightarrow R_1 > 0$. This can be further illustrated in Figure 2.

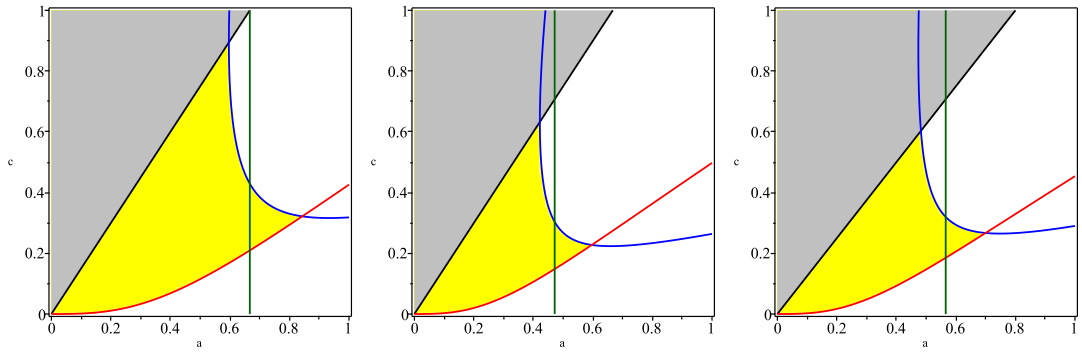

(a) $N = 3$, $k = 1$ (b) $N = 3$, $k = 2$ (c) $N = 5$, $k = 1$

Figure 2: Stability region of model NG1B.

In Figure 2, we present cross-sections of the stability region for model NG1B. The yellow regions indicate the stable parameter regions, while the grey areas correspond to infeasible parameter values ($q_s^* < 0$). Moreover, the blue curves represent the period-doubling bifurcation loci, the red curves denote the Neimark–Sacker bifurcation loci, and the green straight lines indicate the boundaries of the stability region for the N-firm market (the market is stable on the left side of the green line).

One can see that increasing either the number of firms N or the output adjustment speed k causes the stability region to shrink, thereby reducing the overall stability of the system. Furthermore, model NG1B may lose its stability via two possible routes: period-doubling and Neimark–Sacker bifurcations, which will be confirmed by the numerical simulations presented

later. The bifurcation behaviors of model NG1B are qualitatively distinct from those of model NG1G, where only period-doubling bifurcations can occur.

Remark 2. From Figure 2, one can see that if the marginal cost c of the entrant is too small relative to the average marginal cost a of the incumbent firms, the stability region of model NG1B with $N+1$ firms may become significantly smaller than that of the original N-firm model. This occurs because model NG1B may lose stability through a Neimark–Sacker bifurcation. However, when the ratio a/c remains within a moderate range greater than 1, the stability region of model NG1B with $N+1$ firms can in fact exceed that of the original N-firm model.

The economic implication of these results is that, when the entrant adopts the best response mechanism, market stability improves if the entrant's marginal cost is moderately lower (but not excessively lower) than the incumbents' average marginal cost. However, this conclusion differs from that of model NG1G. A plausible explanation is that the best response mechanism enables a firm to reach its target output in one shot. When the entrant is too efficient, such instantaneous adjustment may induce an overreaction, thereby undermining market stability. □

Also, we establish the following corollary. It indicates that if the marginal cost c of the entrant is not too small relative to the average marginal cost a of the N incumbent firms, model NG1B will not undergo Neimark–Sacker bifurcations.

Corollary 1. *Let $a \leq 3c/2$. The equilibrium of model NG1B is locally stable if $R_1 > 0$. Furthermore, period-doubling bifurcations may occur when $R_1 = 0$, but Neimark–Sacker bifurcations cannot take place.*

Proof. The condition $R_2 > 0$ can be rewritten as

$$-(aN+c)(aN-c)((a-2c)N+c)k + 2N^2c > 0. \tag{7}$$

Clearly, $aN + c > 0$. Under the feasible parameter condition $a/c > (N-1)/N$ and $N \geq 2$, we have

$$aN - c > (N-1)c - c = (N-2)c \geq 0.$$

Moreover, from $a \leq 3c/2$ and $N \geq 2$, it follows that

$$(a-2c)N + c \leq -\frac{cN}{2} + c \leq 0.$$

Hence,

$$-(aN+c)(aN-c)((a-2c)N+c) \geq 0,$$

which implies that (7) is always satisfied. The proof is completed. □

3.3 Entry of an LMA firm

Suppose that the entrant adopts the LMA mechanism [11, 27]. The rationality of an LMA entrant is more bounded compared to that of a best responder. Specifically, an LMA firm does not know the exact form of the demand function.[2] However, the LMA entrant can observe the slope of the inverse demand function in the previous period t, i.e., $P'(t) = -1/Q^2(t)$. Accordingly, the entrant can form a linear estimate of the product price according to

$$P^e(t+1) = \frac{1}{Q(t)} - \frac{1}{Q^2(t)}\big(Q^e(t+1) - Q(t)\big),$$

where $Q^e(t+1) = q_s(t+1) + Q_N^e(t+1)$ denotes the entrant's expectation of the market supply for the current period $t+1$.

Moreover, we assume that the entrant employs naive expectations to estimate the output of the incumbent firms, i.e.,

$$Q_N^e(t+1) = Q_N(t),$$

which implies that

$$Q^e(t+1) - Q(t) = q_s(t+1) - q_s(t).$$

Therefore, the entrant estimates the product price for period $t+1$ as

$$P^e(t+1) = \frac{1}{Q(t)} - \frac{1}{Q^2(t)}\big(q_s(t+1) - q_s(t)\big).$$

Then, the expected profit of the entrant is given by

$$\Pi^e(t+1) = q_s(t+1)\left(\frac{1}{Q(t)} - \frac{1}{Q^2(t)}\big(q_s(t+1) - q_s(t)\big)\right) - c\,q_s(t+1).$$

[2]This assumption is reasonable under the condition of nonlinear market demand.

The first-order condition for maximizing the above profit function is

$$\frac{\partial \Pi^e(t+1)}{\partial q_s(t+1)} = \left(\frac{1}{Q(t)} - \frac{1}{Q^2(t)}\big(q_s(t+1) - q_s(t)\big)\right) - \frac{q_s(t+1)}{Q^2(t)} - c = 0,$$

and the second-order condition is always satisfied since

$$\frac{\partial^2 \Pi^e(t+1)}{\partial q_s^2(t+1)} = -\frac{2}{Q^2(t)} < 0.$$

Solving the first-order condition yields

$$q_s(t+1) = \frac{q_s(t) + Q(t) - c\,Q^2(t)}{2}.$$

Recall that $Q = Q_N + q_s$. The new model with $N+1$ firms, which we call model NG1L, can be formulated as the following map:

$$\begin{cases} Q_N(t+1) = Q_N(t) + k\left(\dfrac{N}{Q_N(t)+q_s(t)} - \dfrac{Q_N(t)}{(Q_N(t)+q_s(t))^2} - aN\right), \\ q_s(t+1) = \dfrac{2q_s(t) + Q_N(t) - c(Q_N(t)+q_s(t))^2}{2}. \end{cases} \tag{8}$$

By setting $Q_N(t+1) = Q_N(t) = Q_N^*$ and $q_s(t+1) = q_s(t) = q_s^*$, we obtain the equilibrium equations as follows:

$$\begin{cases} Q_N^* = Q_N^* + k\left(\dfrac{N}{Q_N^*+q_s^*} - \dfrac{Q_N^*}{(Q_N^*+q_s^*)^2} - aN\right), \\ q_s^* = \dfrac{2q_s^* + Q_N^* - c(Q_N^*+q_s^*)^2}{2}. \end{cases}$$

Solving the above equilibrium equations produces the same equilibrium point as models NG1G and NG1B, namely

$$Q_N^* = \frac{cN^2}{(aN+c)^2}, \quad q_s^* = \frac{N\,(aN+c-cN)}{(aN+c)^2}.$$

The Jacobian matrix of map (8) is given by

$$\mathbf{J} = \begin{bmatrix} 1 + k\left(-\dfrac{N+1}{(Q_N(t)+q_s(t))^2} + \dfrac{2Q_N(t)}{(Q_N(t)+q_s(t))^3}\right) & k\left(-\dfrac{N}{(Q_N(t)+q_s(t))^2} + \dfrac{2Q_N(t)}{(Q_N(t)+q_s(t))^3}\right) \\ \dfrac{1}{2} - c\big(Q_N(t)+q_s(t)\big) & 1 - c\big(Q_N(t)+q_s(t)\big) \end{bmatrix}.$$

By evaluating at the equilibrium (Q_N^*, q_s^*), $\mathbf{J}$ can be transformed into

$$\mathbf{J}^* = \begin{bmatrix} 1 - \dfrac{k\big((aN-c)N+aN+c\big)(aN+c)}{N^2} & -\dfrac{k(a^2N^2-c^2)}{N} \\ \dfrac{aN-2cN+c}{2aN+2c} & \dfrac{aN-cN+c}{aN+c} \end{bmatrix}.$$

The two eigenvalues of $\mathbf{J}^*$ are $\frac{\alpha_2 \pm \sqrt{\beta_2}}{2N^2(aN+c)}$, where

$$\begin{aligned}\alpha_2 = & -N^4a^3k - N^3a^3k - N^3a^2ck - 3\,N^2a^2ck + N^2ac^2k - 3\,Nac^2k + Nc^3k + 2\,N^3a - N^3c \\ & - c^3k + 2\,N^2c,\end{aligned}$$

and

$$\begin{aligned}\beta_2 = & N^8a^6k^2 + 2\,N^7a^6k^2 + 2\,N^7a^5ck^2 + N^6a^6k^2 + 8\,N^6a^5ck^2 - N^6a^4c^2k^2 + 6\,N^5a^5ck^2 \\ & + 10\,N^5a^4c^2k^2 - 4\,N^5a^3c^3k^2 - 2\,N^7a^4k + 2\,N^7a^3ck + 15\,N^4a^4c^2k^2 - N^4a^2c^4k^2 \\ & - 6\,N^6a^3ck + 2\,N^6a^2c^2k + 20\,N^3a^3c^3k^2 - 10\,N^3a^2c^4k^2 + 2\,N^3ac^5k^2 - 6\,N^5a^2c^2k \\ & - 2\,N^5ac^3k + 15\,N^2a^2c^4k^2 - 8\,N^2ac^5k^2 + N^2c^6k^2 - 2\,N^4ac^3k - 2\,N^4c^4k + 6\,Nac^5k^2 \\ & - 2\,Nc^6k^2 + N^6c^2 + c^6k^2.\end{aligned}$$

Determining the local stability by directly examining whether the above two eigenvalues lie inside the unit circle is rather cumbersome. However, by applying Jury's criterion, we can establish the following theorem.

Theorem 3. *The equilibrium of model NG1L is locally stable if $R_3 > 0$, where*

$$R_3 = -\left(3a\,N^2 + 4Na - 5Nc + 4c\right)(Na+c)^2\,k + 4\,((2a-c)\,N + 2c)\,N^2.$$

Furthermore, the equilibrium may undergo period-doubling bifurcations when $R_3 = 0$.

Proof. We verify the three conditions given in Lemma 1 sequentially and obtain

$$CD_1 = \frac{(aN+c)^2k}{2N}, \quad CD_2 = \frac{R_3}{2N^2c}, \quad CD_3 = \frac{(Na+c)^2(N^2a+2Na-3Nc+2c)k + 2N^3c}{2N^2c}.$$

Clearly, $CD_1 > 0$ always holds. Moreover, $CD_2 > 0$ is equivalent to $R_3 > 0$. According to

the feasible parameter condition $a/c \geq (N-1)/N$, we have

$$N^2a + 2Na - 3Nc + 2c \geq N\left(\frac{(N+2)(N-1)}{N} - 3\right)c + 2c = N(N-2)c \geq 0,$$

which implies

$$(Na+c)^2(N^2a + 2Na - 3Nc + 2c)k + 2N^3c > 0.$$

Thus, $CD_3 > 0$ always holds.

In short, the equilibrium is locally stable if $R_3 > 0$. The statements regarding bifurcations follow directly from the classic bifurcation theory. The proof is complete. □

Theorem 3 reveals that model NG1L can lose its local stability only through period-doubling bifurcations, which is similar to model NG1G but different from model NG1B. This feature can be observed in Figure 3.

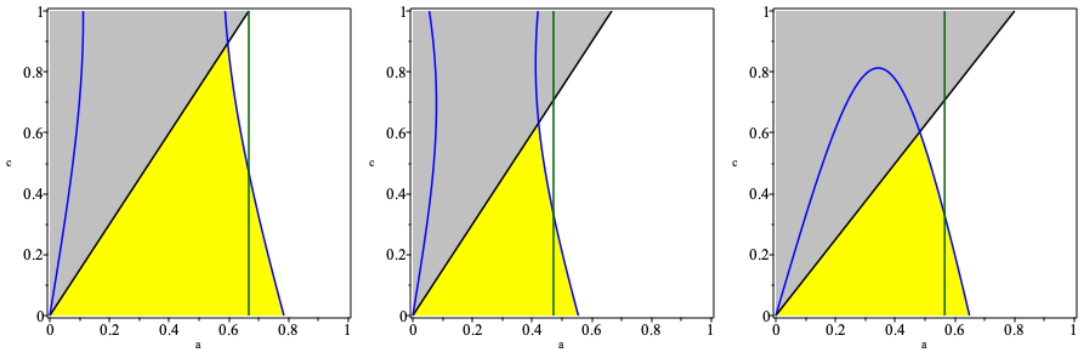

(a) $N = 3$, $k = 1$ (b) $N = 3$, $k = 2$ (c) $N = 5$, $k = 1$

Figure 3: Stability region of model NG1L.

Figure 3 presents several cross-sections of the stability region for model NG1L, where the yellow areas indicate stable regions and the grey areas correspond to infeasible parameter values ($q_s^* < 0$). The blue curves represent period-doubling bifurcation loci, while the green lines denote the boundaries of the stability region for the market with N incumbent firms (the market is stable on the left side of the green lines).

Remark 3. Similar to model NG1G, one can see that when the entrant's marginal cost c is sufficiently low relative to the incumbents' average marginal cost a, the $(N+1)$-firm market may exhibit greater stability than the original N-firm market. The economic implication is that, given that the entrant adopts the LMA mechanism, a sufficiently efficient entrant can enhance

overall market stability.

Notably, similar to the best response mechanism, the LMA mechanism is grounded in the principle of expected-profit maximization. However, because the LMA mechanism relies on an estimated price function, it induces more moderate adjustments. Consequently, an LMA entrant does not overreact even when its efficiency is very high, thereby preventing the destabilizing effects observed in the best response case. □

4 Comparisons

In this section, we compare the stability conditions of the three models (i.e., NG1G, NG1B, and NG1L) derived in the previous section. Table 1 summarizes these stability conditions.

Table 1: **Conditions for local stability of the three models**

model	**stability conditions**
NG1G	$k < \frac{2N}{(aN+c)^2}$
NG1B	$R_1 \equiv (Na+c)\left(a(a-4c)N^2 - 2c(a-2c)N - 3c^2\right)k + 4N^2c > 0$ $R_2 \equiv -(Na+c)(Na-c)((a-2c)N+c)k + 2N^2c > 0$
NG1L	$R_3 \equiv -\left(3aN^2 + 4Na - 5Nc + 4c\right)(Na+c)^2 k + 4((2a-c)N+2c)N^2 > 0$

Under reasonable assumptions, we derive the inclusion relationships among the corresponding stability regions. See Propositions 2 and 3 for further details.

Proposition 2. *Let $a \leq 3c/2$. If model NG1B is locally stable, then model NG1L is locally stable.*

Proof. Since $a \leq 3c/2$, according to Corollary 1, the stability condition of model NG1B is given by $R_1 > 0$, which can be rewritten as

$$k < \frac{4N^2c}{(Na+c)\left(-a(a-4c)N^2 + 2c(a-2c)N + 3c^2\right)}. \tag{9}$$

According to Theorem 3, the stability condition of model NG1L, i.e., $R_3 > 0$, can be rewritten as

$$k < \frac{4((2a-c)N+c)N^2}{(3N^2a + 4Na - 5Nc + 4c)(Na+c)^2}. \tag{10}$$

The calculation shows that

$$\frac{4\left(\left(2a-c\right)N+c\right)N^2}{\left(3N^2a+4Na-5Nc+4c\right)\left(Na+c\right)^2}-\frac{4N^2c}{\left(Na+c\right)\left(-a\left(a-4c\right)N^2+2c\left(a-2c\right)N+3c^2\right)}$$
$$=\frac{8N^2\left(\left(a-2c\right)N+c\right)\left(Na-c\right)\left(\left(a-c\right)N+c\right)}{\left(Na+c\right)^2\left(a\left(a-4c\right)N^2-2c\left(a-2c\right)N-3c^2\right)\left(3N^2a+4Na-5Nc+4c\right)}.$$

Next, we will prove that the right-hand side of the above expression is nonnegative.

We first examine the numerator. From $a \leq 3c/2$ and $N \geq 2$, it follows that

$$\left(a-2c\right)N+c \leq -\frac{cN}{2}+c \leq 0.$$

Moreover, under the feasible parameter condition $a/c \geq (N-1)/N$, we have

$$Na-c \geq (N-2)c \geq 0, \quad (a-c)N+c \geq (N-1)c-Nc+c=0.$$

Hence, the numerator is nonpositive.

Next, we consider the denominator. We rewrite the factor $a\left(a-4c\right)N^2-2c\left(a-2c\right)N-3c^2$ as

$$\left(N^2r^2+(-4N^2-2N)r+4N-3\right)c^2,$$

where $r=a/c$. One can derive that

$$N^2r^2+(-4N^2-2N)r+4N-3<0$$

if and only if

$$\frac{2N+1-2\sqrt{N^2+1}}{N}<r<\frac{2N+1+2\sqrt{N^2+1}}{N}.$$

Under the assumption, we know $(N-1)/N \leq r \leq 3/2$. It is straightforward to verify that

$$\left[\frac{N-1}{N},\frac{3}{2}\right] \subset \left(\frac{2N+1-2\sqrt{N^2+1}}{N},\frac{2N+1+2\sqrt{N^2+1}}{N}\right).$$

Therefore, we obtain

$$a\left(a-4c\right)N^2-2c\left(a-2c\right)N-3c^2<0.$$

Furthermore, under the feasible parameter condition $a/c \geq (N-1)/N$, we have

$$3N^2a + 4Na - 5Nc = N(3Na + 4a - 5c) \geq N\left(\frac{(3N+4)(N-1)}{N} - 5\right)c = (3N^2 - 4N - 4)c.$$

Since $N \geq 2$, it follows that $3N^2 - 4N - 4 \geq 0$. Hence,

$$3N^2a + 4Na - 5Nc + 4c \geq 4c > 0.$$

Consequently, the denominator is negative.

In summary, we have shown that

$$\frac{4\big((2a-c)N+c\big)N^2}{\big(3N^2a + 4Na - 5Nc + 4c\big)(Na+c)^2} - \frac{4N^2c}{(Na+c)\big(-a(a-4c)N^2 + 2c(a-2c)N + 3c^2\big)} \geq 0,$$

which means that the stability condition (9) implies (10). This completes the proof. □

In Proposition 2, the condition $a \leq 3c/2$ is crucial. If this condition is not satisfied, the conclusion of the proposition no longer holds. For example, when $N = 2$, $k = 0.99$, $a = 0.755$, and $c = 0.5$, we have $a/c = 1.51 > 3/2$. In this case,

$$R_1 \approx 0.00080099 > 0, \quad R_2 \approx 3.97990201 > 0, \quad R_3 \approx -0.076357904 < 0,$$

which means that the stability of model NG1B does not imply the stability of model NG1L.

Both Bischi et al. [11] and Naimzada and Tramontana [12] systematically studied the stability of the LMA adjustment mechanism under isoelastic demand. Their analyses are based on the assumption that all firms in their model employ homogeneous adjustment rules. Bischi et al. [11] showed that, compared with best response dynamics, the LMA dynamics require less information while exhibiting stronger local stability. Naimzada and Tramontana [12] established an even stronger result, namely that in the case of duopolistic competition, the LMA mechanism is globally stable.

In contrast, the analysis in Proposition 2 is performed under the assumption that firms employ heterogeneous adjustment mechanisms. The conclusions of Proposition 2 regarding heterogeneous firms are consistent with those by Bischi et al. [11] and Naimzada and Tramontana [12] for homogeneous firms, namely that the LMA mechanism exhibits greater stability than the

best response mechanism. Therefore, within the context of heterogeneous adjustment mechanisms, we also find that less information may lead to more stability.

Proposition 3. *Let $a \leq 3c/2$ and $N \geq 4$. If model NG1L is locally stable, then model NG1G is locally stable.*

Proof. According to Theorem 3, the stability condition $R_3 > 0$ for model NG1L can be rewritten as

$$k < \frac{4\big((2a-c)N+c\big)N^2}{\big(3N^2a+4Na-5Nc+4c\big)(Na+c)^2}, \tag{11}$$

whereas, according to Theorem 1, the stability condition for model NG1G is

$$k < \frac{2N}{(aN+c)^2}. \tag{12}$$

The calculation shows that

$$\frac{2N}{(aN+c)^2} - \frac{4\left((2a-c)N+c\right)N^2}{\left(3N^2a+4Na-5Nc+4c\right)(Na+c)^2} = -\frac{2N\left((a-2c)N+c\right)(N-4)}{\left(3N^2a+4Na-5Nc+4c\right)(Na+c)^2}.$$

Since $a \leq 3c/2$ and $N \geq 4$, we have

$$(a-2c)N + c \leq -cN/2 + c \leq -c < 0.$$

Next, we will prove that $3N^2a + 4Na - 5Nc + 4c > 0$. Under the feasible parameter condition $a/c \geq (N-1)/N$, it follows that

$$3N^2a + 4Na - 5Nc = N(3Na + 4a - 5c) \geq N\left(\frac{(3N+4)(N-1)}{N} - 5\right)c = (3N^2 - 4N - 4)c.$$

Since $N \geq 4$, we have $3N^2 - 4N - 4 > 0$. Hence,

$$3N^2a + 4Na - 5Nc + 4c > 4c > 0.$$

In summary, we derive

$$\frac{2N}{(aN+c)^2} - \frac{4\big((2a-c)N+c\big)N^2}{\big(3N^2a+4Na-5Nc+4c\big)(Na+c)^2} \geq 0,$$

which means that the stability condition (11) implies (12). This completes the proof. □

In Proposition 3, both conditions $a \leq 3c/2$ and $N \geq 4$ are crucial. If either condition is violated, the conclusion of the proposition no longer holds. For example, when $N = 2$, $k = 1.9$, $a = 0.5$, and $c = 0.5$, we have $a/c = 1 < 3/2$. In this case, one can see that $R_3 \approx 2.075 > 0$, but the stability condition (5) is not satisfied, indicating that $N \geq 4$ is critical. Similarly, when $N = 5$, $k = 0.179$, $a = 1.40625$, and $c = 0.5$, we have $a/c = 2.8125 > 3/2$. Here, $R_3 \approx 6.5 > 0$, but the stability condition (5) is again not satisfied, indicating that $a \leq 3c/2$ is also critical.

In model NG1G, the entrant adopts a gradient adjustment mechanism, whereas in model NG1L, the entrant follows the LMA mechanism. Comparing the information requirements of these two types of firms, we find that the gradient firm only needs to know its own marginal profit in the previous period, whereas the LMA firm must know the derivative of the price function with respect to market supply in the previous period. Intuitively, the gradient-adjusting firm relies on less information than the LMA firm. In this sense, Proposition 3 also indicates that less information may lead to greater stability, which is consistent with the main findings of Bischi et al. [11] and Naimzada and Tramontana [12].

Combining Propositions 2 and 3, under the conditions that the marginal cost of the entrant is not too different from the average marginal cost of incumbents (i.e., $(N-1)/N \leq a/c \leq 3/2$)[3] and the number of incumbents is not smaller than four (i.e., $N \geq 4$), we derive the inclusion relationships among the stability regions for the three models. By abuse of notation, their stability regions are ordered as

$$\text{model NG1B} \preceq \text{model NG1L} \preceq \text{model NG1G}.$$

Figure 4 illustrates this result, where two representative cases, $N = 5$, $k = 0.5$ and $N = 10$, $k = 1.0$, are plotted. The stability regions of models NG1B, NG1L, and NG1G are marked in yellow, green, and blue, respectively.

The above analysis shows that, when $(N-1)/N \leq a/c \leq 3/2$ and $N \geq 4$, the homogeneous

[3]In much of the existing literature, firms are often assumed to share identical marginal costs. This assumption greatly simplifies the analytical derivations while still delivering many insightful economic implications. In our framework, this cost-homogeneity assumption corresponds to the special case $a = c$, where the entrant's marginal cost c coincides with the incumbents' average marginal cost a. Our assumption $a/c \leq 3/2$ can therefore be viewed as a natural extension of the benchmark case $a = c$. Although our assumption does not allow for scenarios in which entrants have extremely low costs, we believe it encompasses a broad class of practically relevant situations where entrants and incumbents exhibit only "moderate" cost differences.

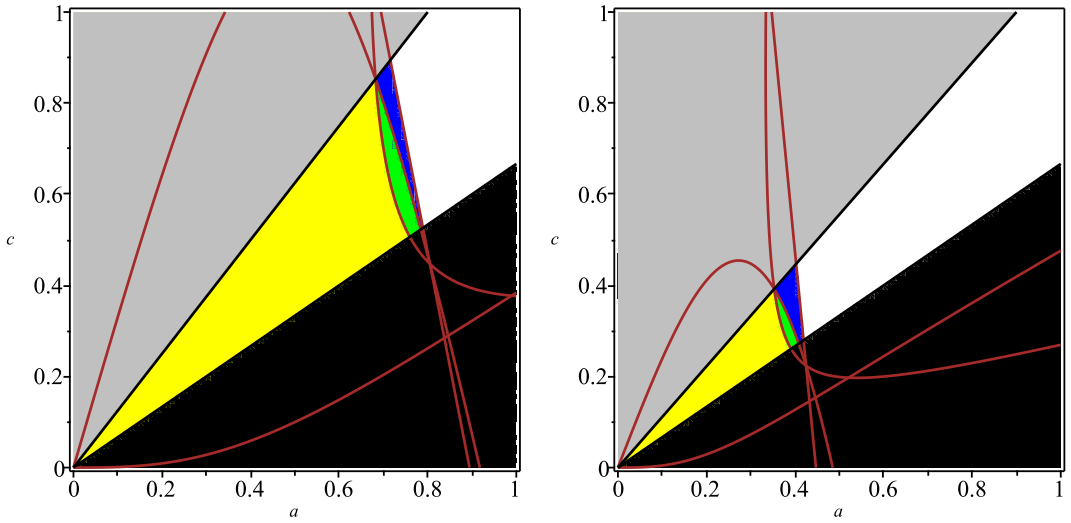

(a) $N = 5$, $k = 0.5$ (b) $N = 10$, $k = 1.0$

Figure 4: Comparison of the stability regions of the three models. The infeasible parameter region is marked in grey, while the region satisfying $a > 3c/2$ is highlighted in black. The yellow, green, and blue regions represent the stability regions of models NG1B, NG1L, and NG1G, respectively.

oligopoly model (model NG1G) exhibits stronger stability than the heterogeneous oligopoly models (models NG1B and NG1L). This conclusion contrasts with that of Tramontana et al. [15]. By gradually introducing heterogeneous firms, Tramontana et al. examined duopolistic, triopolistic, and quadrupolistic market structures, and their study suggests that heterogeneity in firms' decision-making mechanisms may enhance market stability. Analyzing the reasons for the discrepancy between our findings and those of Tramontana et al. is beyond the scope of this paper and is left for future research.

Furthermore, with respect to bifurcations, the analysis given in Section 3 reveals that model NG1B behaves differently from the other two models, which is further confirmed by the numerical simulations presented in the following section.

5 Numerical Simulations

In this section, we perform numerical simulations for models NG1G, NG1B, and NG1L. The simulation results confirm the theoretical bifurcation analysis presented in Section 3: models NG1G and NG1L may undergo period-doubling bifurcations, while model NG1B can exhibit both period-doubling and Neimark–Sacker bifurcations. Moreover, we find that model NG1B

may also experience degenerate Neimark–Sacker bifurcations, corresponding to resonance cases such as 1:3, 1:4, and 1:5.

Figure 5(a) presents a one-dimensional bifurcation diagram of model NG1G with respect to the parameter a, where the other parameters are set as $N = 3$, $k = 1$, and $c = 0.2$. The initial state for the iterations is chosen as $(Q_N(0), q_s(0)) = (0.3, 0.9)$. In the diagram, the trajectories of $Q_N(t)$ and $q_s(t)$ are marked in red and blue, respectively. Moreover, Figure 5(b) depicts the maximum Lyapunov exponent of model NG1G, thereby offering a quantitative indicator of chaotic dynamics.

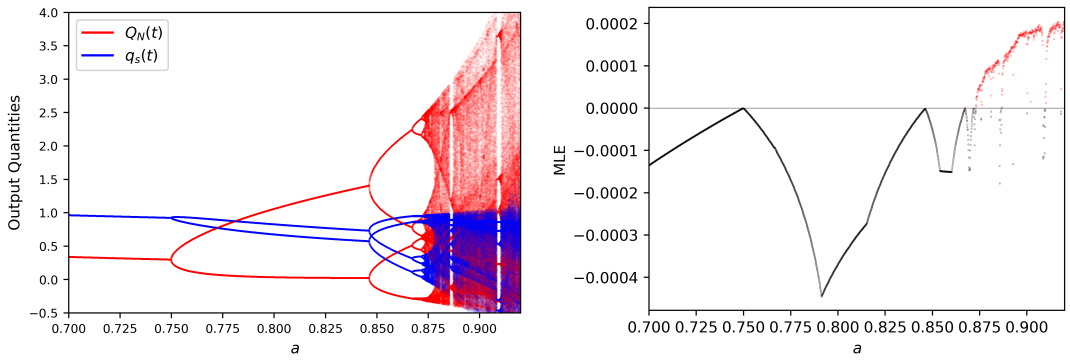

(a) (b)

Figure 5: (a) The one-dimensional bifurcation diagram of model NG1G with respect to a. The trajectories $Q_N(t)$ and $q_s(t)$ are marked in red and blue, respectively. (b) The maximum Lyapunov exponent (MLE) of model NG1G as a varies. The other parameters are selected as $N = 3$, $k = 1$, and $c = 0.2$. The initial state is chosen as $(Q_N(0), q_s(0)) = (0.3, 0.9)$.

From Figure 5(a), we observe a cascade of period-doubling bifurcations leading to chaos, a phenomenon commonly referred to as the Feigenbaum scenario. When the parameter a is sufficiently small, the trajectory converges to a stable equilibrium. As the parameter a increases, the system undergoes a period-doubling bifurcation at the critical value $a \approx 0.749024512256128$. At this point, a stable fixed point (period-1 orbit) loses its stability as one of the eigenvalues of the Jacobian matrix crosses -1 on the real axis. Beyond this critical value, a stable period-2 orbit emerges, represented by two alternating branches in the bifurcation diagram. With further increases in a, successive period-doubling bifurcations occur ($2 \to 4 \to 8 \to \cdots$). For instance, the period-2 orbit transitions to a period-4 orbit at $a \approx 0.8459479739869935$, to a period-8 orbit at $a \approx 0.8673336668334166$, and to a period-16 orbit at $a \approx 0.8718359179589794$. Eventually, when a becomes sufficiently large, the system exhibits chaotic dynamics.

In Figure 6, we present several one-dimensional bifurcation diagrams of model NG1B with

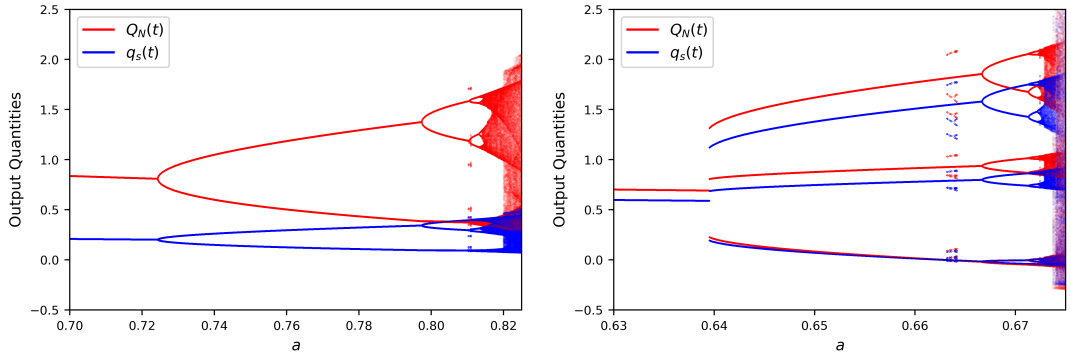

(a) (b)

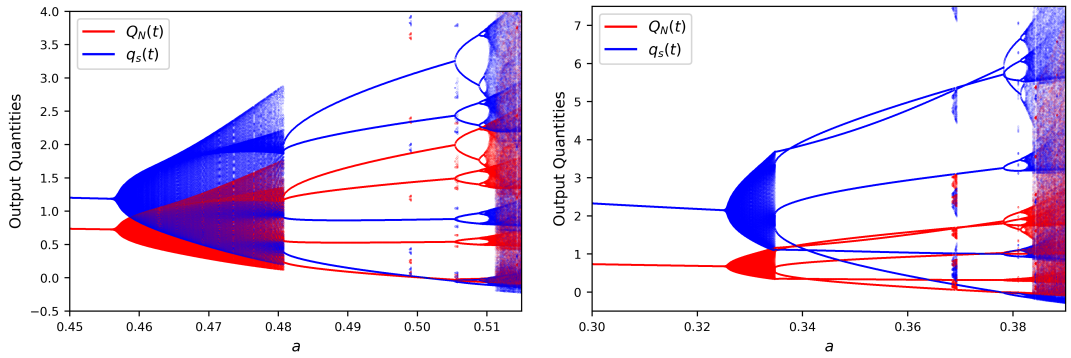

(c) (d)

Figure 6: The one-dimensional bifurcation diagrams of model NG1B with respect to a, where $N = 3$ and $k = 1$. The trajectories $Q_N(t)$ and $q_s(t)$ are marked in red and blue, respectively. (a) Period-doubling bifurcations with $c = 0.4$ and $(Q_N(0), q_s(0)) = (1.0, 0.3)$. (b) 1:3 resonance bifurcations with $c = 0.27$ and $(Q_N(0), q_s(0)) = (0.5, 0.86)$. (c) 1:4 resonance bifurcations with $c = 0.19$ and $(Q_N(0), q_s(0)) = (0.64, 1.19)$. (d) 1:5 resonance bifurcations with $c = 0.12$ and $(Q_N(0), q_s(0)) = (0.88, 1.82)$.

respect to the parameter a, where the other parameters are set as $N = 3$ and $k = 1$. By choosing different values of c, we observe distinct bifurcation behaviors. For example, in Figure 6(a), we fix $c = 0.4$ and select the initial state $(Q_N(0), q_s(0)) = (1.0, 0.3)$, under which a typical period-doubling bifurcation is observed. Similar to Figure 5(a), the trajectory in Figure 6(a) first converges to an equilibrium, and successive period-doubling bifurcations occur ($2 \to 4 \to 8 \to \cdots$) as the parameter a increases.

In Figure 6(b), we fix $c = 0.27$ and choose the initial state $(Q_N(0), q_s(0)) = (0.5, 0.86)$. From this one-dimensional bifurcation diagram, a 1:3 resonance bifurcation can be clearly observed. A 1:3 resonance bifurcation occurs when the eigenvalues of the Jacobian matrix at the fixed point lie on the unit circle and satisfy the condition

$$\lambda_{1,2} = \mathrm{e}^{\pm \mathrm{i}\frac{2\pi}{3}}.$$

At the critical parameter value, the rotation angle of the complex-conjugate pair is approximately 120°, leading to a resonance between the invariant closed curve and a period-3 orbit. In the bifurcation diagram, this phenomenon is manifested by the appearance of a stable or unstable period-3 orbit that becomes locked onto the invariant curve.

Specifically, Figure 6(b) shows that the trajectory converges to a stable equilibrium when the parameter a is small. When $a \approx 0.6391845922961481$, the stable equilibrium suddenly disappears and is replaced by the emergence of a period-3 orbit. When $a \approx 0.666648324162081$, the period-3 orbit undergoes a transition to a period-6 orbit. As the parameter a further increases, period-12 and period-24 orbits appear successively, ultimately giving rise to chaos.

In Figure 7, phase portraits illustrating the process of the 1:3 resonance bifurcation are presented, where the initial state is also set to $(Q_N(0), q_s(0)) = (0.5, 0.86)$. Each phase portrait is generated from 3000 iterations of the system. The first 2000 trajectory points are shown in grey, while the last 1000 points are displayed in black to highlight the asymptotic behaviors. Figure 7(a) demonstrates that the trajectory converges to a stable equilibrium. Figure 7(b) shows the emergence of a period-3 orbit, and Figure 7(c) illustrates a chaotic orbit.

In Figure 6(c), we fix $c = 0.19$ and choose the initial state $(Q_N(0), q_s(0)) = (0.64, 1.19)$. From this one-dimensional bifurcation diagram, we can observe the occurrence of a 1:4 resonance bifurcation. A 1:4 resonance bifurcation takes place when the eigenvalues of the Jacobian matrix

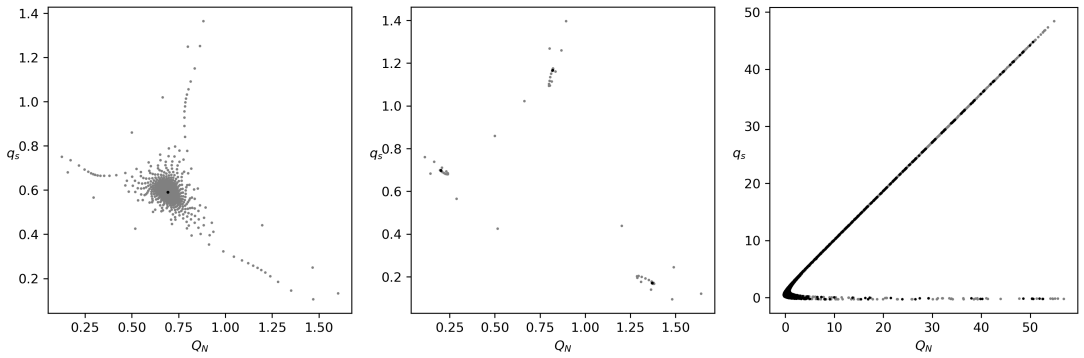

(a) $a = 0.639091$ (b) $a = 0.640303$ (c) $a = 0.676061$

Figure 7: The phase portraits (1:3 resonance) of model NG1B with $N = 3$, $k = 1$, and $c = 0.27$. The initial state is selected as $(Q_N(0), q_s(0)) = (0.5, 0.86)$ and 3000 iterations are conducted. The first 2000 trajectory points are marked in grey, while the last 1000 points are marked in black.

at a fixed point lie on the unit circle and satisfy

$$\lambda_{1,2} = \mathrm{e}^{\pm \mathrm{i}\frac{2\pi}{4}}.$$

Figure 6(c) shows that the trajectory converges to the equilibrium for $a < 0.45544272136068037$. As the parameter a increases, a quasi-periodic orbit (invariant closed curve) emerges. However, when $a \approx 0.4807753876938469$, the invariant closed curve is destroyed and replaced by a period-4 orbit. As a continues to increase, period-8 and period-16 orbits successively appear, eventually leading to chaotic dynamics.

Figure 8 presents phase portraits illustrating the process of the 1:4 resonance bifurcation, where the initial state is also set to $(Q_N(0), q_s(0)) = (0.64, 1.19)$. In Figure 8(a), the trajectory rotates and converges to a stable equilibrium. Figure 8(b) displays a stable invariant closed curve, while Figure 8(c) shows that the shape of the invariant closed curve becomes distorted. In Figure 8(d), the trajectory converges to a period-4 orbit. Figure 8(e) illustrates the emergence of a stable period-8 orbit, and Figure 8(f) depicts a chaotic attractor with a single piece.

In Figure 6(d), we fix $c = 0.12$ and choose the initial state $(Q_N(0), q_s(0)) = (0.88, 1.82)$. From this one-dimensional bifurcation diagram, the occurrence of a 1:5 resonance bifurcation can be observed. A 1:5 resonance bifurcation takes place when the eigenvalues of the Jacobian matrix at a fixed point lie on the unit circle and satisfy the condition

$$\lambda_{1,2} = \mathrm{e}^{\pm \mathrm{i}\frac{2\pi}{5}}.$$

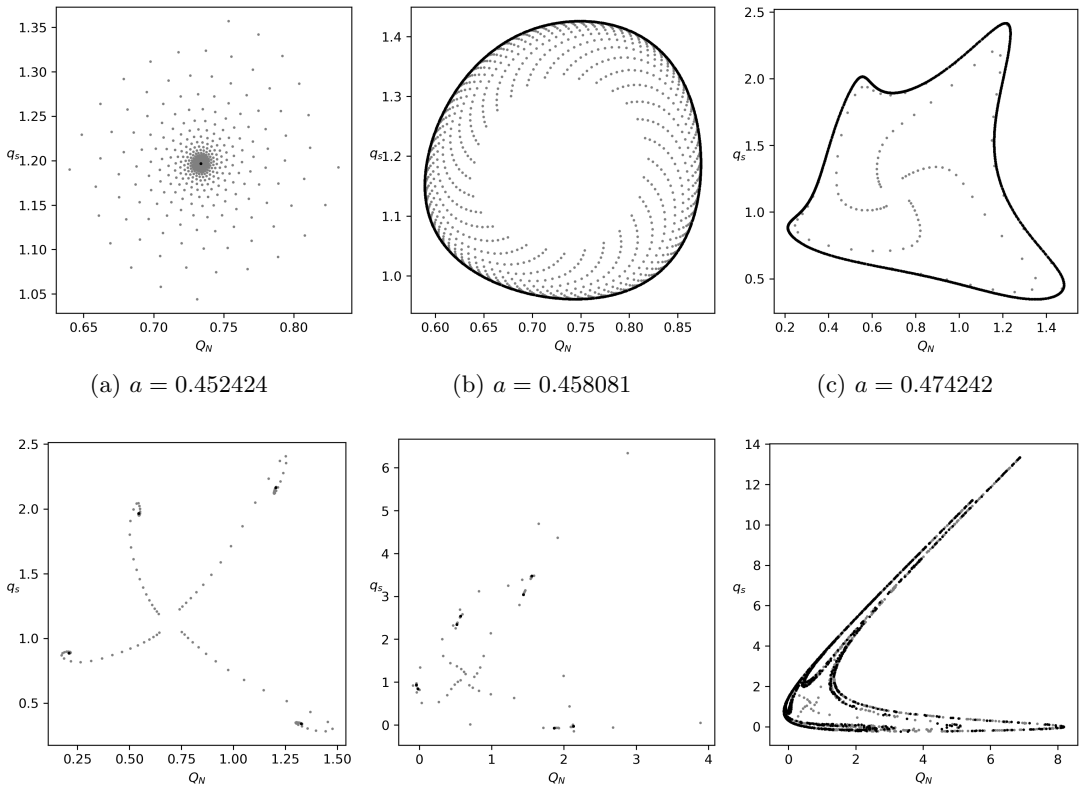

(a) $a = 0.452424$ (b) $a = 0.458081$ (c) $a = 0.474242$

(d) $a = 0.481515$ (e) $a = 0.506566$ (f) $a = 0.515455$

Figure 8: The phase portraits (1:4 resonance) of model NG1B with $N = 3$, $k = 1$, and $c = 0.19$. The initial state is selected as $(Q_N(0), q_s(0)) = (0.64, 1.19)$ and 3000 iterations are conducted. The first 2000 trajectory points are marked in grey, while the last 1000 points are marked in black.

Specifically, Figure 6(d) shows that the trajectory converges to a stable equilibrium for $a < 0.3248074037018509$. As a increases, a stable invariant closed curve emerges. However, when $a \approx 0.3348024012006003$, the invariant closed curve is destroyed and replaced by a stable period-5 orbit. As the parameter a further increases, a period-10 orbit occurs at $a \approx 0.37824912456228116$, and a period-20 orbit appears at $a \approx 0.38144572286143075$. Finally, when a is sufficiently large, the trajectory converges to a strange attractor.

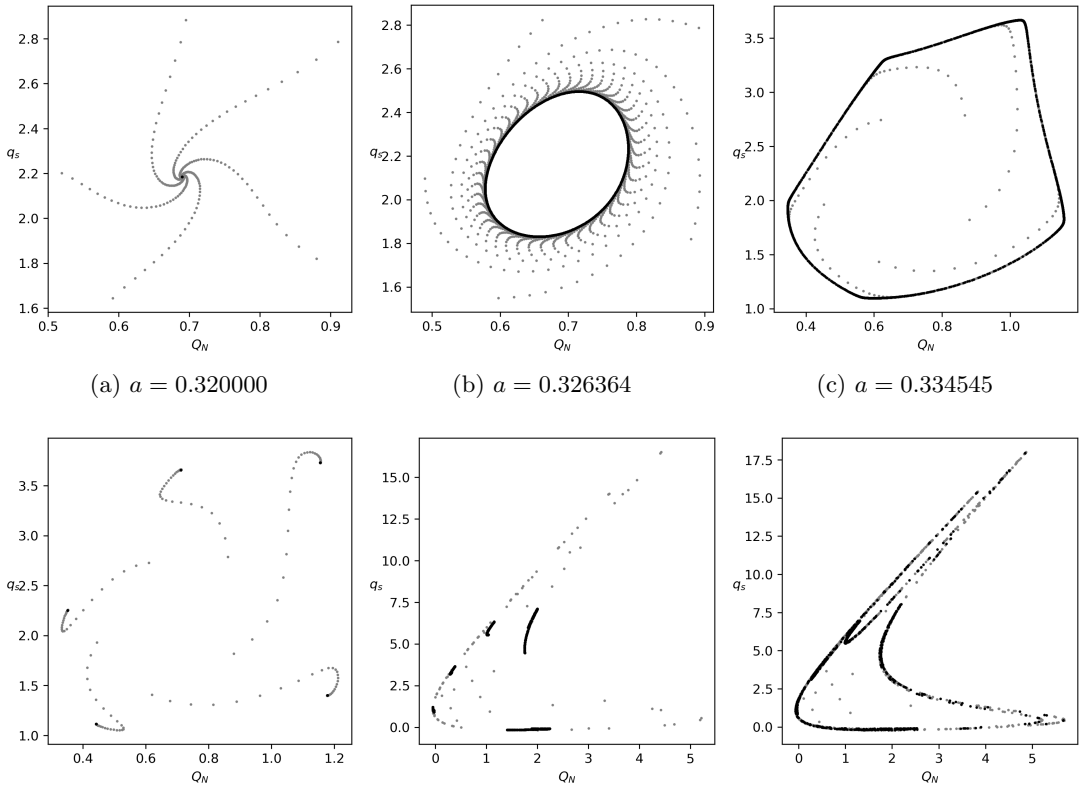

(a) $a = 0.320000$ (b) $a = 0.326364$ (c) $a = 0.334545$

(d) $a = 0.336364$ (e) $a = 0.383636$ (f) $a = 0.385455$

Figure 9: The phase portraits (1:5 resonance) of model NG1B with $N = 3$, $k = 1$, and $c = 0.12$. The initial state is selected as $(Q_N(0), q_s(0)) = (0.88, 1.82)$ and 3000 iterations are conducted. The first 2000 trajectory points are marked in grey, while the last 1000 points are marked in black.

In Figure 9, we present phase portraits illustrating the process of the 1:5 resonance bifurcation, where the initial state is chosen as $(Q_N(0), q_s(0)) = (0.88, 1.82)$. In Figure 9(a), the trajectory converges to a stable equilibrium from five directions. Figure 9(b) shows a stable invariant closed curve, to which the trajectory converges from the outside. As illustrated in Figure 9(c), the shape of the invariant closed curve becomes distorted, and the trajectory approaches it from the inside. In Figure 9(d), the trajectory converges to a period-5 orbit. Figure 9(e) depicts a strange attractor consisting of five pieces, while Figure 9(f) shows a strange

attractor with a single piece.

Moreover, from Figure 6, we observe that the trajectory of model NG1B abruptly departs from the main branch within certain narrow intervals of the parameter a. This arises from the coexistence of multiple attractors. For instance, consider the case corresponding to Figure 6(b) with parameters $N = 3$, $k = 1$, and $c = 0.27$.

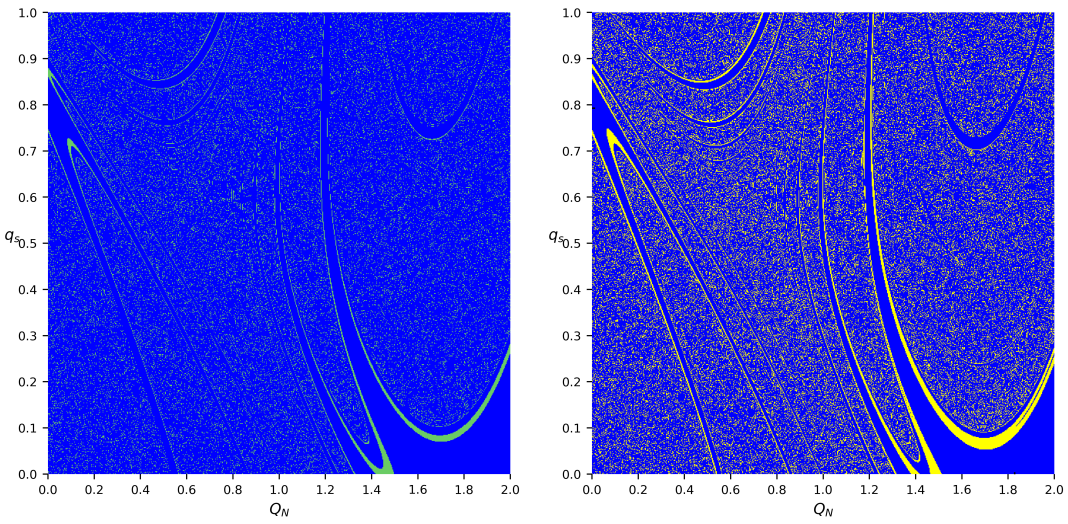

(a) (b)

Figure 10: Basins of attraction for model NG1B with $N = 3$, $k = 1$, and $c = 0.27$. (a) For $a = 0.6632$: the blue region denotes the basin of the period-3 attractor [(-0.001, 0.79), (0.927, 1.545), (1.814, -0.001)], while the green region denotes the basin of the period-9 attractor [(0.092, 0.72), (1.474, -0.01), (2.049, 0.017), (1.032, 1.746), (0.02, 0.72), (0.846, 1.256), (-0.012, 0.879), (1.654, 0.079), (0.845, 1.409)]. (b) For $a = 0.6644$: the blue region denotes the basin of the period-3 attractor [(0.931, 1.558), (-0.007, 0.793), (1.828, -0.006)], while the yellow region denotes the basin of a chaotic attractor.

When $a = 0.6632$, the period-3 attractor [(-0.001, 0.79), (0.927, 1.545), (1.814, -0.001)] coexists with a period-9 attractor. Figure 10(a) illustrates the corresponding basins of attraction: initial conditions marked in blue converge to the period-3 attractor, whereas those in green converge to the period-9 attractor. In contrast, when $a = 0.6644$, the period-3 attractor [(0.931, 1.558), (-0.007, 0.793), (1.828, -0.006)] coexists with a chaotic attractor. Figure 10(b) displays their basins of attraction, where blue points converge to the period-3 attractor and yellow points converge to the chaotic attractor. As illustrated, the basin boundaries exhibit a highly complex topological structure.

For model NG1L, Figure 11(a) presents a one-dimensional bifurcation diagram with respect to the parameter a, where the other parameters are set to $N = 3$, $k = 1$, and $c = 0.2$. The

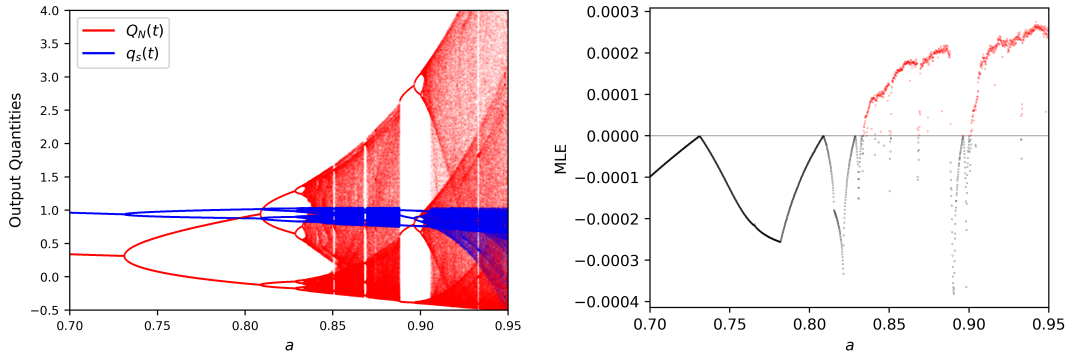

(a) (b)

Figure 11: (a) The one-dimensional bifurcation diagram of model NG1L with respect to a. The trajectories $Q_N(t)$ and $q_s(t)$ are marked in red and blue, respectively. (b) The maximum Lyapunov exponent (MLE) of model NG1L as a varies. The other parameters are selected as $N = 3$, $k = 1$, and $c = 0.2$. The initial state is chosen as $(Q_N(0), q_s(0)) = (0.3, 0.9)$.

initial condition for the iterations is chosen as $(Q_N(0), q_s(0)) = (1.0, 0.4)$. It can be observed that model NG1L loses stability through a cascade of period-doubling bifurcations as the parameter a increases. Eventually, when a is sufficiently large, the system exhibits chaotic dynamics. Figure 11(b) shows the corresponding maximum Lyapunov exponent, which offers a quantitative indicator of chaos.

In Figure 12, we present the one-dimensional bifurcation diagrams of the three models with respect to the parameter c. Figures 12(a), (b), and (d) indicate that all three models may lose stability through period-doubling bifurcations as c increases. In contrast, Figure 12(c) shows that model NG1B may undergo a Neimark–Sacker bifurcation as c decreases.

Figure 13 presents the two-parameter bifurcation diagrams of models NG1G, NG1B, and NG1L. In these diagrams, parameter points corresponding to periodic orbits of different orders are indicated using distinct colors. Notably, regions colored in yellow represent periodic orbits of order greater than or equal to 24, which are associated with complex dynamics, including chaos, quasi-periodic behaviors, or higher-order periodic orbits. Additionally, parameter points where the system's trajectory diverges (approaching infinity) are shaded in grey. For further details on two-dimensional bifurcation diagrams and their computational methods, readers are referred to [28].

These two-dimensional bifurcation diagrams illustrate the qualitative changes in the system's dynamics with respect to the control parameters a and c. In Figures 13(a) and (c), the initial states are set to $(Q_N(0), q_s(0)) = (1.0, 0.4)$. The numerical simulation results for model

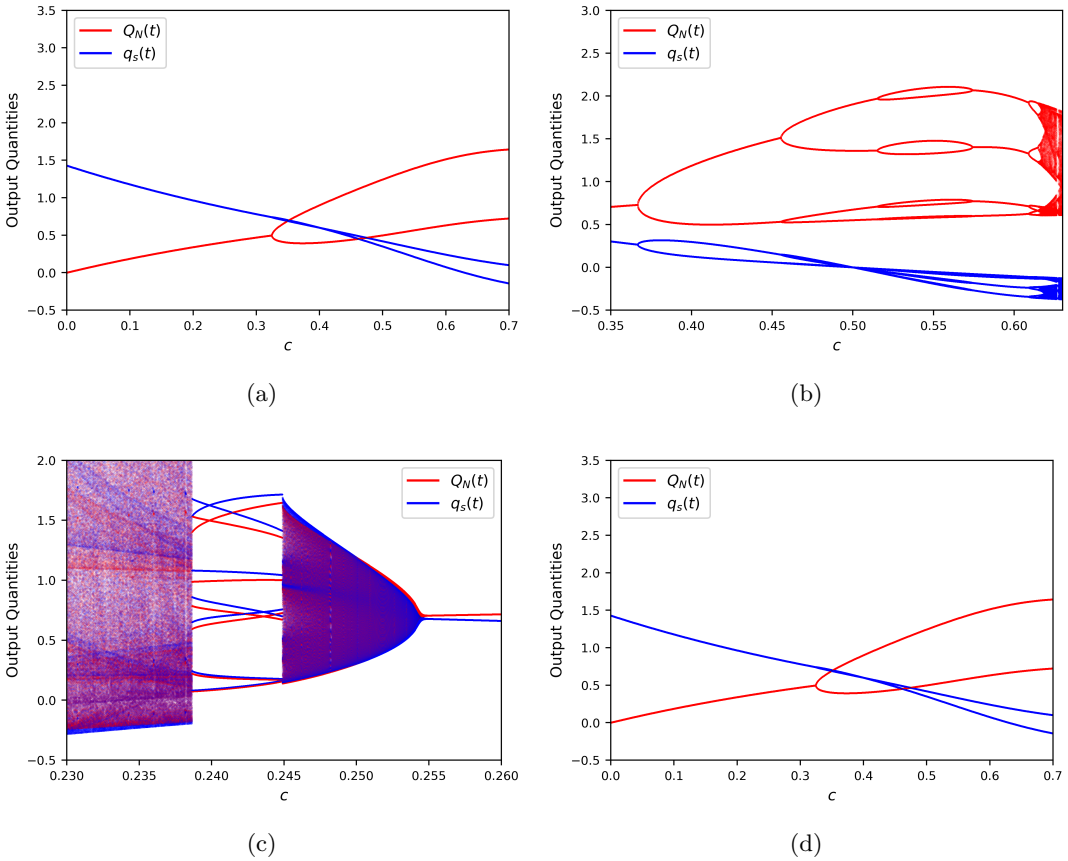

Figure 12: The one-dimensional bifurcation diagrams of the three models with respect to c, where $N = 3$ and $k = 1$. The trajectories $Q_N(t)$ and $q_s(t)$ are marked in red and blue, respectively. (a) Model NG1G with $a = 0.7$ and $(Q_N(0), q_s(0)) = (0.3, 0.9)$. (b) Model NG1B with $a = 0.76$ and $(Q_N(0), q_s(0)) = (0.42, 0.67)$. (c) Model NG1B with $a = 0.6$ and $(Q_N(0), q_s(0)) = (0.42, 0.67)$. (d) Model NG1L with $a = 0.7$ and $(Q_N(0), q_s(0)) = (0.3, 0.9)$.

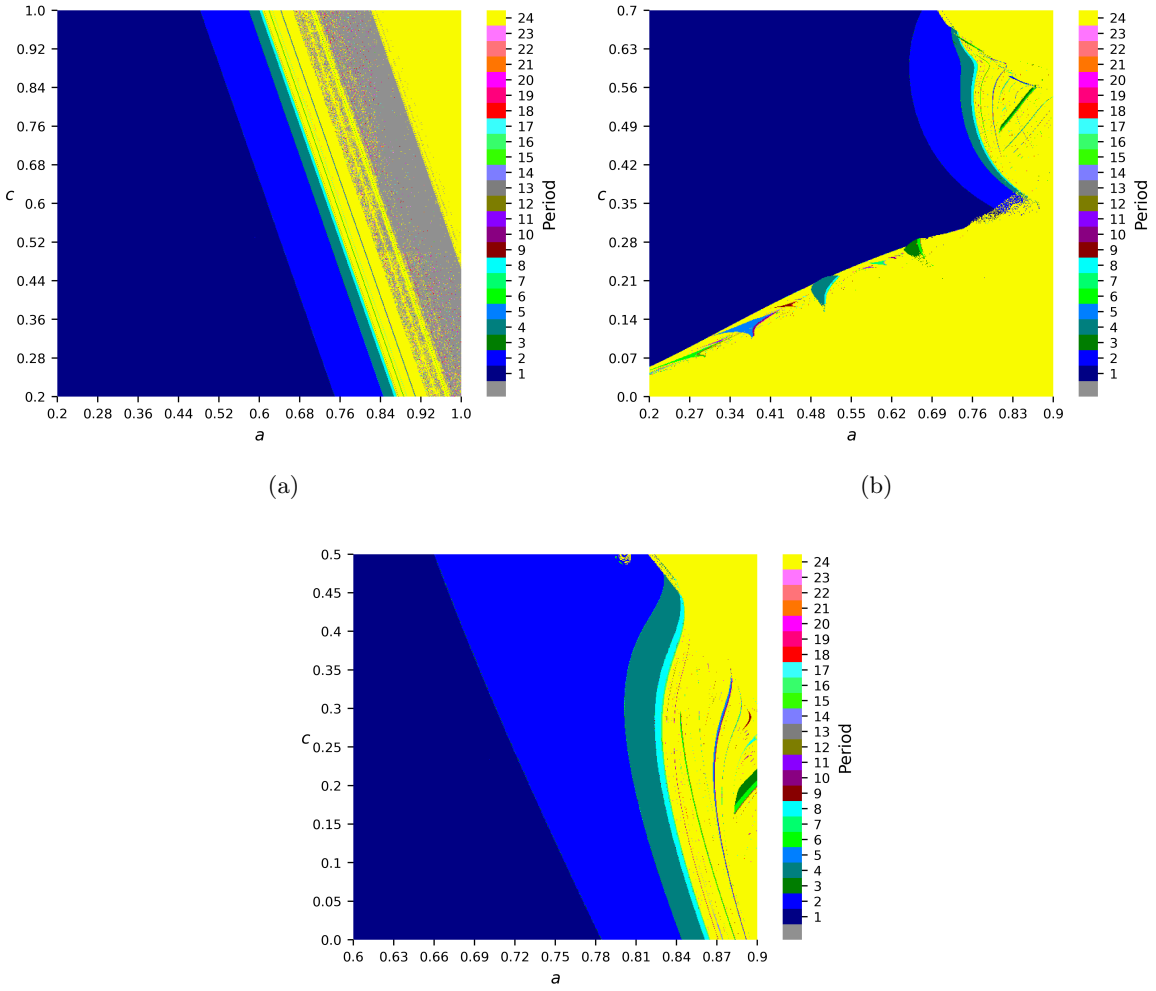

(a) (b)

(c)

Figure 13: The two-dimensional bifurcation diagrams of the three models with respect to a and c, where $N = 3$ and $k = 1$. (a) Model NG1G with $(Q_N(0), q_s(0)) = (1.0, 0.4)$. (b) Model NG1B with $(Q_N(0), q_s(0)) = (0.42, 0.67)$. (c) Model NG1L with $(Q_N(0), q_s(0)) = (1.0, 0.4)$.

NG1G shown in Figure 13(a) are consistent with the analytical results presented in Figure 1(a). For example, as the parameter a or c increases, the equilibrium of model NG1G loses stability through a sequence of period-doubling bifurcations. Similarly, the numerical results for model NG1L shown in Figure 13(c) agree with the analytical results presented in Figure 3(a).

Figure 13(b) illustrates the global bifurcation structure of model NG1B in the parameter space, which not only reveals qualitative changes in the system's behaviors under different parameter combinations but also highlights the interactions among various bifurcation curves. The initial condition is chosen as $(Q_N(0), q_s(0)) = (0.42, 0.67)$. It can be observed that the dynamical behaviors of model NG1B are significantly different from those of the other two models, as it can lose stability through both Neimark–Sacker and period-doubling bifurcations. Moreover, Figure 13(b) explicitly indicates the possible occurrence of degenerate Neimark–Sacker bifurcations, corresponding to 1:3, 1:4, and 1:5 resonance cases.

6 Concluding Remarks

Under a market structure characterized by isoelastic demand and N gradient-adjusting firms, this paper investigates the market-entry problem. We compare the dynamical behaviors that arise when the entrant adopts one of three different output adjustment mechanisms, namely the gradient adjustment, the best response, and the LMA, in order to identify which adjustment rule is more conducive to market stability.

Under the assumptions that the marginal cost of the entrant does not differ significantly from the average marginal cost of the incumbents and that the number of incumbent firms is no less than four, we establish an inclusion relationship among the stability regions of the three entry games: the smallest stability region corresponds to model NG1B, the intermediate one to model NG1L, and the largest to model NG1G. This result is consistent with the existing literature on homogeneous oligopoly models employing best response and LMA mechanisms. Since an LMA firm requires less information than a best response firm, and a gradient-adjusting firm requires even less information than an LMA firm, the above results suggest that less information may lead to more stability.

Regarding bifurcations, we find that model NG1B differs from the other two models. Specifically, models NG1G and NG1L can lose stability only through period-doubling bifurcations,

whereas model NG1B may lose stability through two distinct routes: period-doubling and Neimark–Sacker bifurcations. Numerical simulations confirm this conclusion and further reveal that model NG1B may undergo degenerate Neimark–Sacker bifurcations, such as the 1:3, 1:4, and 1:5 resonance bifurcations. In addition, we discover that model NG1B may display the coexistence of multiple attractors.

In the existing literature, few studies have examined the stability of entry games. To the best of our knowledge, this paper represents the first attempt in this direction. Our study extends the relevant research on dynamic oligopoly games and offers insights for regulators in designing market entry policies. Specifically, the analysis in Section 3 shows that the entry of more efficient, or equivalently lower-cost, firms may enhance the local stability of the equilibrium. Therefore, regulators can apply this finding when designing entry policies for some regulated industries to improve overall market stability.

For analytical simplicity, the present framework considers only the case in which all incumbent firms adopt the gradient adjustment mechanism. Extending this framework by replacing the incumbents' gradient adjustment mechanism with alternative behavioral rules—such as the best response or adaptive mechanism—constitutes an interesting avenue for future research.

Acknowledgments

The authors are grateful to the anonymous referees for their helpful comments. This work was partially supported by Philosophy and Social Science Foundation of Guangdong (Grant No. GD25CLJ03), MoE Key Laboratory of Interdisciplinary Research of Computation and Economics (Shanghai University of Finance and Economics), and Innovation Team Project of Guangdong Colleges and Universities (Grant No. 2024WCXTD019).

References

[1] A. A. Cournot. *Recherches sur les principes mathématiques de la théorie des richesses.* chez L. Hachette, Paris, 1838.

[2] R. D. Theocharis. On the stability of the Cournot solution on the oligopoly problem. *The Review of Economic Studies*, 27(2):133–134, 1960.

[3] F. M. Fisher. The stability of the Cournot oligopoly solution: The effects of speeds of adjustment and increasing marginal costs. *The Review of Economic Studies*, 28(2):125–135, 1961.

[4] M. McManus and R. E. Quandt. Comments on the stability of the Cournot oligipoly model. *The Review of Economic Studies*, 28(2):136–139, 1961.

[5] R. Sato and K. Nagatani. The stability of oligopoly with conjectural variations. *The Review of Economic Studies*, 34(4):409–416, 1967.

[6] J. Hadar. Stability of oligopoly with product differentiation. *The Review of Economic Studies*, 33(1):57–60, 1966.

[7] A. Zhang and Y. Zhang. Stability of a Cournot-Nash equilibrium: The multiproduct case. *Journal of Mathematical Economics*, 26(4):441–462, 1996.

[8] T. Puu. Chaos in duopoly pricing. *Chaos, Solitons & Fractals*, 1(6):573–581, 1991.

[9] G. I. Bischi and M. Kopel. Equilibrium selection in a nonlinear duopoly game with adaptive expectations. *Journal of Economic Behavior & Organization*, 46(1):73–100, 2001.

[10] W. Wu, Z. Chen, and W. H. Ip. Complex nonlinear dynamics and controlling chaos in a Cournot duopoly economic model. *Nonlinear Analysis: Real World Applications*, 11(5):4363–4377, 2010.

[11] G. I. Bischi, A. K. Naimzada, and L. Sbragia. Oligopoly games with local monopolistic approximation. *Journal of Economic Behavior & Organization*, 62(3):371–388, 2007.

[12] A. K. Naimzada and F. Tramontana. Controlling chaos through local knowledge. *Chaos, Solitons & Fractals*, 42(4):2439–2449, 2009.

[13] B. Xin, W. Peng, and Y. Kwon. A discrete fractional-order Cournot duopoly game. *Physica A: Statistical Mechanics and its Applications*, 558:124993, 2020.

[14] H. N. Agiza and A. A. Elsadany. Nonlinear dynamics in the Cournot duopoly game with heterogeneous players. *Physica A: Statistical Mechanics and its Applications*, 320:512–524, 2003.

[15] F. Tramontana, A. A. Elsadany, B. Xin, and H. N. Agiza. Local stability of the Cournot solution with increasing heterogeneous competitors. *Nonlinear Analysis: Real World Applications*, 26:150–160, 2015.

[16] F. Cavalli and A. K. Naimzada. A Cournot duopoly game with heterogeneous players: Nonlinear dynamics of the gradient rule versus local monopolistic approach. *Applied Mathematics and Computation*, 249:382–388, 2014.

[17] F. Cavalli, A. K. Naimzada, and M. Pireddu. Heterogeneity and the (de) stabilizing role of rationality. *Chaos, Solitons & Fractals*, 79:226–244, 2015.

[18] A. E. Matouk, A. A. Elsadany, and B. Xin. Neimark–Sacker bifurcation analysis and complex nonlinear dynamics in a heterogeneous quadropoly game with an isoelastic demand function. *Nonlinear Dynamics*, 89(4):2533–2552, 2017.

[19] A. A. Elsadany and A. M. Awad. Dynamics and chaos control of a duopolistic Bertrand competitions under environmental taxes. *Annals of Operations Research*, 274(1-2):211–240, 2019.

[20] S. Ng. Looking for evidence of speculative stockholding in commodity markets. *Journal of Economic Dynamics and Control*, 20(1):123–143, 1996.

[21] B. Adrangi and A. Chatrath. Non-linear dynamics in futures prices: Evidence from the coffee, sugar and cocoa exchange. *Applied Financial Economics*, 13:245–256, January 2003.

[22] J. Andaluz, A. A. Elsadany, and G. Jarne. Dynamic Cournot oligopoly game based on general isoelastic demand. *Nonlinear Dynamics*, 99(2):1053–1063, 2020.

[23] X. Li, B. Li, and L. Liu. Stability and dynamic behaviors of a limited monopoly with a gradient adjustment mechanism. *Chaos, Solitons & Fractals*, 168:113106, 2023.

[24] W. Yu and Y. Yu. A dynamic duopoly model with bounded rationality based on constant conjectural variation. *Economic Modelling*, 37:103–112, 2014.

[25] X. Li and L. Su. Local stability and convergence factors of nonlinear duopoly games with different types of players. *Nonlinear Dynamics*, 112(19):17627–17648, 2024.

[26] E. I. Jury, L. Stark, and V. V. Krishnan. Inners and stability of dynamic systems. *IEEE Transactions on Systems, Man, and Cybernetics*, (10):724–725, 1976.

[27] X. Li, J. Yang, and A. Q. Zhang. Influence of price elasticity of demand on monopoly games under different returns to scale. *Mathematics and Computers in Simulation*, 233:75–98, 2025.

[28] W. Marszalek, H. Podhaisky, and J. Sadecki. Computing two-parameter bifurcation diagrams for oscillating circuits and systems. *IEEE Access*, 7:115829–115835, 2019.